

## Electric-field-sustained spiral waves in subexcitable media

Mei-chun Cai, Jun-ting Pan, and Hong Zhang\*

*Zhejiang Institute of Modern Physics and Department of Physics, Zhejiang University, Hangzhou 310027, China*

(Received 20 November 2011; revised manuscript received 5 April 2012; published 10 July 2012)

We present numerical evidence that, in the presence of a suitable electric field, an isolated broken plane wave retracting originally in subexcitable media can propagate continuously and eventually evolve into a rotating spiral. Simulations for the FitzHugh-Nagumo, the Barkley, and the Oregonator models are carried out and the same electric-field-sustained spiral phenomena are observed. Semianalytical results in the framework of a kinematic theory are quantitatively consistent with the numerical results.

DOI: [10.1103/PhysRevE.86.016208](https://doi.org/10.1103/PhysRevE.86.016208)

PACS number(s): 89.75.Kd, 82.40.Ck, 47.54.-r

### I. INTRODUCTION

Spiral waves are ubiquitous in various biological, chemical, and physical systems. They have been observed in cardiac tissue [1], during aggregation of *Dictyostelium discoideum* amoebae [2], in the Belousov-Zhabotinsky (BZ) reaction [3,4], in catalytic oxidation of CO [5], etc. The attractiveness of investigating the dynamics of spiral waves is not only because they have a special structure, i.e., the core is regarded as a phase singularity in mathematical language, but more importantly they also contribute to an underlying class of cardiac diseases, such as tachycardia and fibrillation [6–8].

In recent years, spatiotemporal pattern formation in subexcitable media has gained extensive attention. In these systems, the medium excitability is sufficient for a plane wave to propagate but not for a rotating spiral to form, and the end of a broken plane wave simply retracts steadily [9,10]. Jung and Mayer-Kress [11,12] first proposed the concept of spatiotemporal stochastic resonance, showing noise can sustain spiral growth in a subexcitable medium. Besides spiral waves [13,14], noise can also stabilize propagating wave segments [15], induce driven avalanche behavior [16], and sustain pulsating patterns and global oscillations [17] in subexcitable media. The propagating wave segment that has two free ends is inherently unstable in subexcitable media, but can also be stabilized by periodic modulation of [18] and feedback to the medium excitability [19–21]. Zykov and Showalter [22] point out that the existence of stabilized propagating wave segments can be understood by considering the interaction of the wave front and wave back boundaries.

In Ref. [23], the authors show that electric noise can sustain propagating waves in subexcitable media at an optimal level of noise. Electric fields are known to have pronounced effects on the behaviors of spiral waves in excitable media. Both dc and ac electric fields can induce the drift of spirals [24–27]. Recently, a circularly polarized electric field (CPEF) has been proposed theoretically [28,29], and the drift of spiral waves under the influence of such an electric field is studied numerically. By applying two ac electric fields perpendicular to each other with four electrodes (see Fig. 1), the CPEF has been realized in the Belousov-Zhabotinsky (BZ) reaction experimentally [30]. Tuning the phase difference between

those two perpendicular fields, one can produce a clockwise ( $\pi/2$ ) or a counterclockwise ( $3\pi/2$ ) rotating CPEF. In this paper, we report our numerical study on the influence of CPEFs on an isolated broken plane wave in subexcitable media. We observe that the broken wave no longer shrinks, but evolves into a rotating spiral under the influence of a CPEF with suitable amplitude and frequency. Moreover, semianalytical interpretation, in the framework of a kinematic theory [10], for this phenomenon is also discussed, and the obtained results are quantitatively consistent with the numerical ones.

### II. NUMERICAL RESULTS

We consider the following FitzHugh-Nagumo (FHN) model submitted to an external electric field  $\mathbf{E}$  [31]:

$$\partial_t u = \varepsilon \nabla^2 u + f(u, v) / \varepsilon - \mathbf{E} \cdot \nabla u, \quad \partial_t v = g(u, v), \quad (1)$$

where  $f(u, v) = 3u - u^3 - v$  and  $g(u, v) = u - \delta \cdot u$  and  $v$  are the fast activator and the slow inhibitor, respectively.  $\varepsilon$  and  $\delta$  are parameters characterizing the excitability of the medium. Through this paper,  $\mathbf{E} = (E_x, E_y)$  is a counterclockwise rotating CPEF, where  $E_x = E_0 \cos(\omega_e t)$ ,  $E_y = E_0 \cos(\omega_e t + 3\pi/2)$ , where  $E_0$  is the amplitude of the electric field and  $\omega_e$  is its angular frequency (see Fig. 1). In our numerical simulation, we choose  $(\varepsilon, \delta) = (0.2, -1.432)$ , which is in the subexcitable parameter region close to the  $\partial R$  boundary, i.e., the boundary between subexcitable and excitable media [10].

Figure 2 shows the propagation of an isolated broken plane wave in the system without and with CPEFs. For the CPEF-free system, the excitation wave shrinks and disappears eventually [see Figs. 2(a)–2(c)], which is a typical characteristic of a broken plane wave in subexcitable media. However, the behavior of the wave would change dramatically once a suitable CPEF is applied to the system. For instance, Figs. 2(d)–2(f) show typical snapshots of a broken plane wave propagating continuously in the presence of a CPEF with  $E_0 = 0.2$  and  $\omega_e = 0.2$ . The excitation wave does not shrink any more but continues to propagate and eventually evolves into a spiral which rotates rigidly in the same direction with the CPEF.

Further study for a large range of the amplitude  $E_0$  and the frequency  $\omega_e$  shows that the dynamical behaviors of excitation waves crucially depend on the chosen CPEF parameters. As shown in the phase diagram (see Fig. 3), with different  $E_0$  and  $\omega_e$ , the excitation waves perform different behaviors. Specifically, within the so-called “rigidly rotating spiral” region in the phase diagram, the broken plane wave can be

\*Author to whom correspondence should be addressed: hongzhang@zju.edu.cn

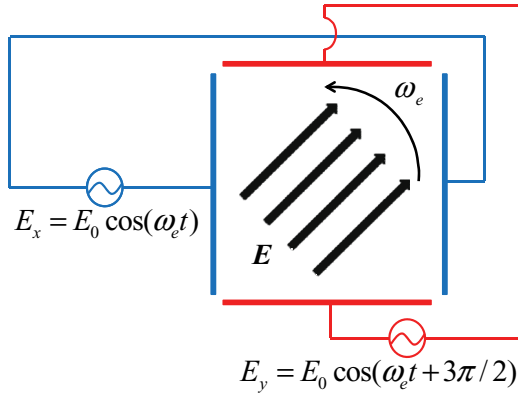


FIG. 1. (Color online) Realization sketch of a counterclockwise rotating circularly polarized electric field (CPEF). Applying two ac electric fields with the phase difference  $3\pi/2$  perpendicular to each other, one can get a counterclockwise CPEF.

forced to form a rigidly rotating spiral, whose frequency is identical to that of the CPEF, i.e., the spiral rotates synchronously with the CPEF [see Fig. 2(f)]. The rigidly rotating spiral appears when the amplitude  $E_0 \geq 0.05$  and the frequency  $\omega_e$  is around 0.03. Numerical results show that when we further increase the amplitude  $E_0$ , the range of  $\omega_e$  for the rigidly rotating spiral will be extended. What is more, for the case of both  $E_0$  and  $\omega_e$  being fixed in this region, the angle between the tip tangential velocity  $c_t$  and the electric field  $E$ ,  $\theta$  [refer to Fig. 6(a)], stays constant all the time [see Fig. 4(a)], while for varied  $E_0$  and  $\omega_e$ , the angle  $\theta$  will be different accordingly [e.g., see Figs. 4(c) and 4(d)].

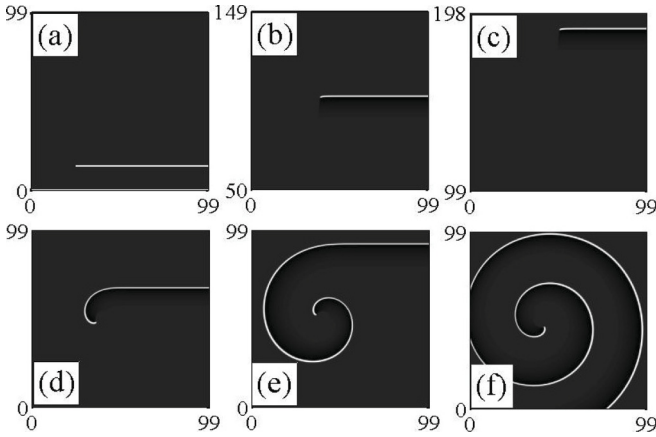


FIG. 2. The evolution of an isolated broken plane wave in the subexcitable system without and with CPEFs in Eq. (1). The top row shows the case of no CPEF [integration of Eq. (1) without the gradient term  $E \cdot \nabla u$ ] at (a)  $t = 0$ , (b)  $t = 99$ , (c)  $t = 198$ . The system consists of  $1500 \times 3000$  grid points. The bottom row exhibits the case that the broken plane wave is forced to form a rigidly rotating spiral by a CPEF with  $E_0 = 0.2$  and  $\omega_e = 0.2$  at (d)  $t = 26$ , (e)  $t = 53$ , (f)  $t = 97$ . The system is comprised of  $1500 \times 1500$  grid points. The Euler algorithm with the space step  $\Delta x = \Delta y = 0.066$  and time step  $\Delta t = 0.0044$  is employed to integrate Eq. (1). No-flux conditions are imposed at the boundaries. Hereafter, in the integration of Eq. (1), the same simulation method and parameters applied in (d)–(f) will be used in this paper.

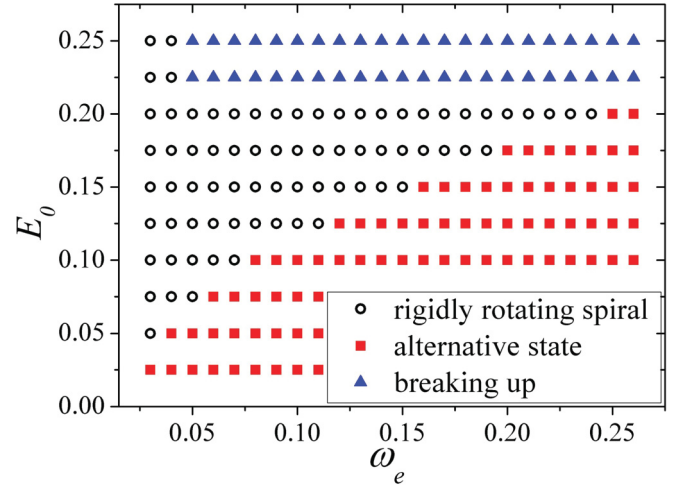


FIG. 3. (Color online) The phase diagram in the  $E_0 - \omega_e$  plane of Eq. (1). The steps of  $E_0$  and  $\omega_e$  are 0.025 and 0.01, respectively.

In the “alternative state” region, the excitation wave neither rotates permanently nor retracts steadily, but rotates and retracts alternately [for a specific example one can refer to Fig. 7(a)]. Compared with the case of the “rigidly rotating spiral” region, where  $\theta$  stays constant over time [see Fig. 4(a)],  $\theta$  here changes periodically as time elapses [see Fig. 4(b)]. This means the tip tangential velocity  $c_t$  cannot catch up with the rotating electric field  $E$  any more, then the angle between them changes periodically over time.

In the “breaking up” region, the excitation wave breaks up far away from the tip when the electric field strength is above a threshold value  $E_c$ . Furthermore, from the detailed phase diagram of the “breaking up” region (see Fig. 5), we find that the threshold value  $E_c$  increases with the electric field frequency  $\omega_e$ .

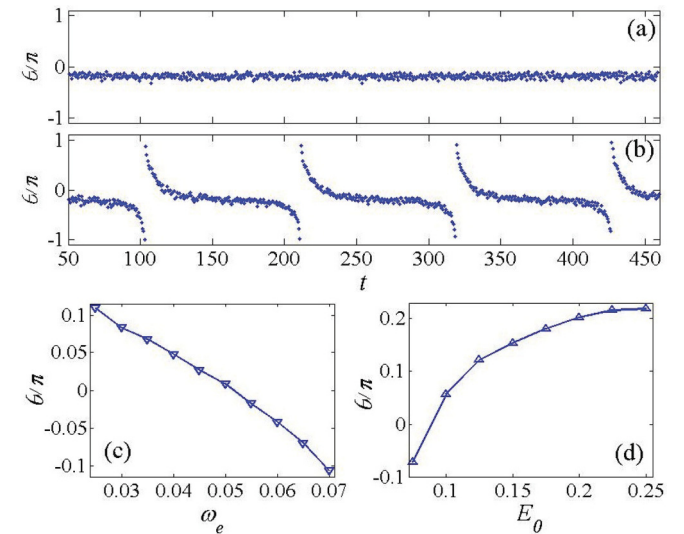


FIG. 4. (Color online)  $\theta$  properties in the “rigidly rotating spiral” region (a), (c), (d), and the “alternative state” region (b). The CPEF parameters are (a)  $E_0 = 0.2$ ,  $\omega_e = 0.236$ ; (b)  $E_0 = 0.2$ ,  $\omega_e = 0.244$ ; (c)  $E_0 = 0.1$ ; and (d)  $\omega_e = 0.04$ .

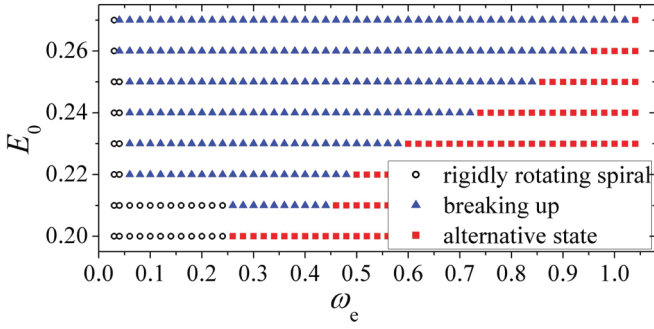


FIG. 5. (Color online) The detailed phase diagram of the “breaking up” region in the  $E_0 - \omega_e$  plane of Eq. (1). The steps of  $E_0$  and  $\omega_e$  are 0.01 and 0.02, respectively.

### III. MECHANISM

At present, the breakup of excitation waves in the presence of intensive electric field has been observed in the BZ reaction, and its corresponding mechanism has also been discussed [32,33], and our findings about the breaking up of the excitation wave agree with the results. In the following, we will reveal the mechanism of the rigidly rotating spirals and the alternative state in the subexcitable media under the influence of CPEFs.

In Ref. [34], a kinematical model of wave motion close to the  $\partial R$  boundary (the boundary between subexcitable and excitable media) is proposed on a phenomenological basis and has been helpful to rationalize experimental facts. In Ref. [10], an asymptotic derivation of a kinematic theory of wave motion close to the  $\partial R$  boundary is presented and has been developed to describe rotating spiral waves, critical fingers, and retracting fingers. The kinematic description has provided exact predictions for the drift of spiral waves affected by dc electric fields. In the following, we attempt to explain our numerical results using this kinematic theory.

Close to the  $\partial R$  boundary, in the absence of any external field, the tip tangential speed  $c_t$  of an isolated broken plane wave can be expressed as [10]

$$c_t = c_0 + c_B, \quad (2)$$

where  $c_0$  is the plane wave speed;  $c_B = c_0(B - B_c)/K$ , in which  $K \approx 0.63$  is a numerical constant;  $B = 4\sqrt{3}\varepsilon/\Delta^3$  characterizes the excitability of the medium, with  $\Delta = \delta^3 - 3\delta$ ; and  $B_c = 0.535$  is a critical value which distinguishes the subexcitable media ( $B > B_c$ ) from the excitable ones ( $B < B_c$ ). Namely, if  $B = B_c$ , i.e.,  $c_t = c_0$ , the tip of a broken plane wave would never extend or retract, which is called “critical finger”; and if  $B > B_c$ , i.e.,  $c_t > c_0$ , the excitation wave propagates forward. Meanwhile, its tip retracts as shown in the top row of Fig. 2, and it is named “retracting finger”; only if  $B < B_c$ , i.e.,  $c_t < c_0$ , can the excitation wave rotate to be a spiral. With the chosen parameters  $\varepsilon = 0.2$  and  $\delta = -1.432$ , according to Eq. (2), we can have  $B = 0.5515$  and thus  $B > B_c$ , i.e.,  $c_t > c_0$ .

In the presence of a weak electric field  $\mathbf{E}$ , Eq. (2) can be reconsidered in a frame  $M$  moving at velocity  $\mathbf{E}$  and modified as [10]

$$c_t = c_0 + c_B + c_E. \quad (3)$$

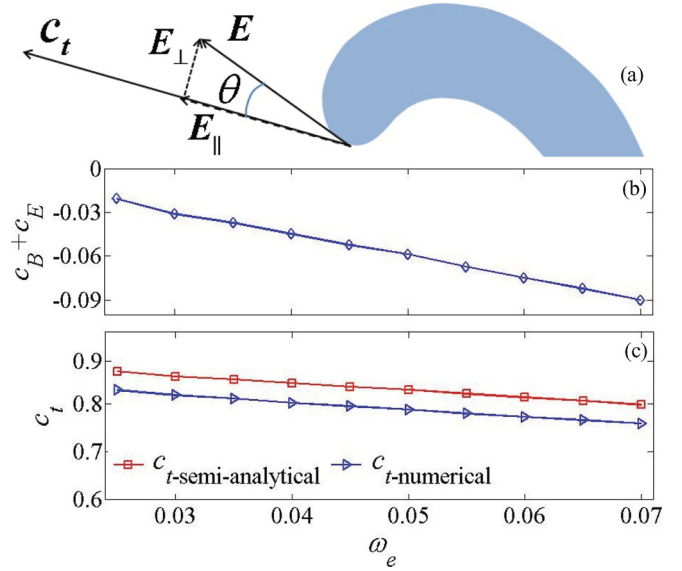


FIG. 6. (Color online) (a) The sketch of a wave tip submitted to a CPEF. (b) Results of  $c_B + c_E$  varying with  $\omega_e$ . (c) The comparison of  $c_{t\text{-semi-analytical}}$  and  $c_{t\text{-numerical}}$  in the frame  $M$ . Both (b) and (c) are performed within the “rigidly rotating spiral” region shown in Fig. 3 with  $E_0 = 0.1$ .

Here,  $c_E = \gamma_{\parallel} E_{\parallel} + \gamma_{\perp} E_{\perp}$ , in which  $E_{\perp} = E_0 \sin \theta$  and  $E_{\parallel} = E_0 \cos \theta$  are the external field components, respectively, parallel and orthogonal to  $\mathbf{c}_t$ .  $\gamma_{\parallel} \approx -0.850$  and  $\gamma_{\perp} \approx 0.929$  are numerical coefficients.  $\theta$  is the angle between  $\mathbf{c}_t$  and  $\mathbf{E}$  [see Fig. 6(a)].

In the following, we show that the above observed wave behaviors under the influence of CPEFs can be attributed to the change of the tip tangential speed  $c_t$  caused by the electric fields. First, we measure  $c_0$  numerically in the subexcitable medium without any external field. For the parameters  $\varepsilon = 0.2$  and  $\delta = -1.432$ , the measured value of  $c_0$  is about 0.8887, and  $c_t$  is about 0.8912, i.e.,  $c_t > c_0$  for the retracting finger [see Figs. 2(a)–2(c)]. Second, in the presence of a CPEF, we measure  $c_t$  and calculate it in the frame  $M$ . The measured value of  $c_t$  in the frame  $M$  is denoted as  $c_{t\text{-numerical}}$ . Third, we numerically measure the value of  $\theta$ , the angle between  $\mathbf{c}_t$  and  $\mathbf{E}$ , then we calculate the value of  $c_E = \gamma_{\parallel} E_0 \cos \theta + \gamma_{\perp} E_0 \sin \theta$  and the value of  $c_B + c_E$  in the frame  $M$ . Finally, we can obtain the value of  $c_t$  according to Eq. (3) and denote it as  $c_{t\text{-semi-analytical}}$ .

Figure 6(b) shows the dependence of  $c_B + c_E$  on  $\omega_e$  in the “rigidly rotating spiral” region for  $E_0 = 0.1$ . One can see that all the values of  $c_B + c_E$  in this region are negative, which means  $c_t < c_0$ . That is to say, after applying the CPEF to the subexcitable system, from Eq. (3), the relation between  $c_t$  and  $c_0$  realizes the transition from  $c_t > c_0$  to  $c_t < c_0$  and the isolated broken plane wave now no longer shrinks, but can evolve into a rotating spiral, which well explains our observed numerical results shown in Figs. 2(d)–2(f) and 3. The values of  $c_t$  measured directly from numerical simulation and the ones obtained from Eq. (3) in the “rigidly rotating spiral” region for  $E_0 = 0.1$  are given in Fig. 6(c). The comparison of the semi-analytical results with the direct numerical ones shows

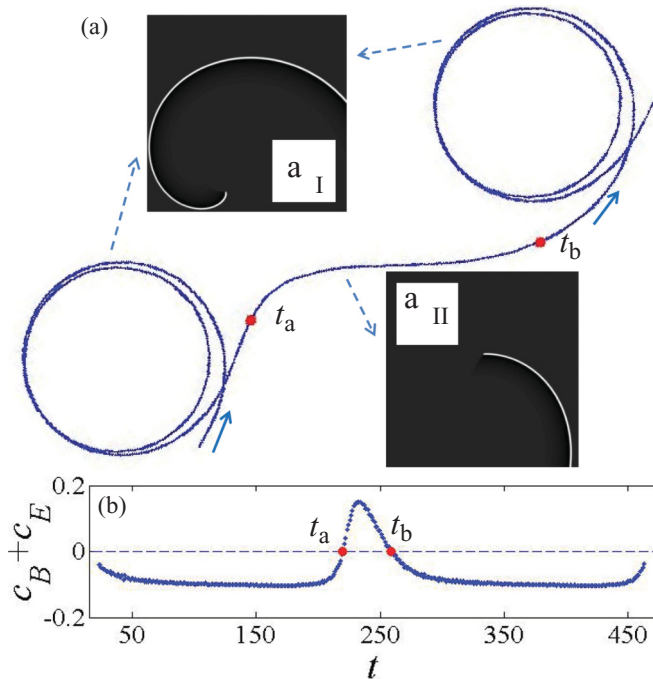


FIG. 7. (Color online) (a) The trajectory of a wave tip affected by a CPEF with  $E_0 = 0.1$  and  $\omega_e = 0.076$  in the “alternating state” region. The snapshot  $a_I$  shows the rotating spiral and  $a_{II}$  shows the retracting finger. (b) Time evolution of the corresponding results of  $c_B + c_E$ .

that there is good agreement even for the case where  $E_0$  is not extremely small (in Ref. [10], the dc electric field  $E = 0.001$ ).

Furthermore, similar analysis based on Eq. (3) can also be applied to interpret the wave dynamical behaviors in the “alternating state” region, where the rotating spiral and the retracting finger arise alternatively. Figure 7(a) shows an “alternating state” case with  $E_0 = 0.1$  and  $\omega_e = 0.076$ . For a rotating spiral, i.e., in the time region  $t \notin [t_a, t_b]$ , the tip trajectory is relatively round and the wave shape around the tip is clearly curly [see Figs. 7(a) and 7( $a_I$ )]. For a retracting finger, i.e., in the time region  $t \in [t_a, t_b]$ , there is a shrinking track in the tip trajectory and the wave shape near the tip is a typical retracting finger (see Figs. 7(a) and 7( $a_{II}$ )).

Correspondingly, the sign of  $c_B + c_E$  which is calculated from Eq. (3) also changes alternatively [see Fig. 7(b)]. Within the time region  $t \in [t_a, t_b]$ ,  $c_B + c_E > 0$  which means  $c_t > c_0$ , and the excitation wave is expected to be a retracting finger. In the other time region  $t \notin [t_a, t_b]$ ,  $c_B + c_E < 0$  which leads to  $c_t < c_0$ , and a rotating spiral is expected theoretically. One can see that all our semianalytical expectations agree entirely with the simulation results.

Our further investigations show that the CPEF-sustained spirals in subexcitable media are also observed in other reaction-diffusion systems, such as the Barkley model [35] and the Oregonator model [36]. The transition from  $c_t > c_0$  to  $c_t < c_0$  is also found in these two models, when the retracting fingers turn into the rotating spirals. We also obtain the phase diagram of the Barkley model, which is similar to that of the FHN model shown in Fig. 3. This indicates that our findings may be model-independent.

#### IV. CONCLUSION

To conclude, the wave behaviors in subexcitable media change greatly once CPEFs are applied to the system. One of the most interesting phenomena, the CPEF-sustained spiral, indicates that the CPEF can support a broken plane wave to propagate continuously and eventually form a rotating spiral. This kind of spiral can be numerically found in the FHN, the Barkley, and the Oregonator models in our present study. In the framework of a kinematic theory [10], we provide semianalytical interpretation for this phenomenon. Finally, we hope CPEF-sustained spirals can be observed in experiments such as the BZ reaction.

#### ACKNOWLEDGMENTS

We thank Qi Ouyang for making valuable comments on this manuscript. This work is supported by the National Nature Science Foundation of China (Grant No. 10975117), the Program for New Century Excellent Talents in University, the Fundamental Research Funds for the Central Universities, and the Soft Matter Research Center of Zhejiang University. M.C.C. and J.T.P. contributed equally to this work.

- 
- [1] J. M. Davidenko, A. V. Pertsov, R. Salomonsz, W. Baxter, and J. Jalife, *Nature (London)* **355**, 349 (1992).  
 [2] K. J. Lee, E. C. Cox, and R. E. Goldstein, *Phys. Rev. Lett.* **76**, 1174 (1996).  
 [3] A. T. Winfree, *Science* **175**, 634 (1972).  
 [4] V. K. Vanag and I. R. Epstein, *Science* **294**, 835 (2001).  
 [5] S. Jakubith, H. H. Rotermund, W. Engel, A. von Oertzen, and G. Ertl, *Phys. Rev. Lett.* **65** 3013 (1990).  
 [6] R. A. Gray, A. M. Pertsov, and J. Jalife, *Nature (London)* **392**, 75 (1998).  
 [7] F. X. Witkowski, L. J. Leon, P. A. Penkoske, W. R. Giles, M. L. Spano, W. L. Ditto, and A. T. Winfree, *Nature (London)* **392**, 78 (1998).  
 [8] S. Luther, F. H. Fenton, B. G. Kornreich, A. Squires, P. Bittihn, D. Hornung, M. Zabel, J. Flanders, A. Gladuli, L. Campoy, E. M. Cherry, G. Luther, G. Hasenfuss, V. I. Krinsky, A. Pumir, R. F. Gilmour Jr, and E. Bodenschatz, *Nature (London)* **475**, 235 (2011).  
 [9] A. S. Mikhailov and V. S. Zykov, *Physica D (Amsterdam, Neth.)* **52**, 379 (1991).  
 [10] See V. Hakim and A. Karma, *Phys. Rev. E* **60**, 5073 (1999), and references therein.  
 [11] P. Jung and G. Mayer-Kress, *Phys. Rev. Lett.* **74**, 2130 (1995).  
 [12] P. Jung and G. Mayer-Kress, *Chaos* **5**, 458 (1995).  
 [13] P. Jung, A. Cornell-Bell, F. Moss, S. Kadar, J. Wang, and K. Showalter, *Chaos* **8**, 567 (1998).

- [14] S. Alonso, F. Sagues, and J. M. Sancho, *Phys. Rev. E* **65**, 066107 (2002).
- [15] S. Kádár, J. Wang, and K. Showalter, *Nature (London)* **391**, 770 (1998).
- [16] J. Wang, S. Kádár, P. Jung, and K. Showalter, *Phys. Rev. Lett.* **82**, 855 (1999).
- [17] H. Hempel, L. Schimansky-Geier, and J. Garcia-Ojalvo, *Phys. Rev. Lett.* **82**, 3713 (1999).
- [18] I. Sendiña-Nadal, E. Mihaliuk, J. Wang, V. Pérez-Muñuzuri, and K. Showalter, *Phys. Rev. Lett.* **86**, 1646 (2001).
- [19] E. Mihaliuk, T. Sakurai, F. Chirila, and K. Showalter, *Phys. Rev. E* **65**, 065602(R) (2002).
- [20] T. Sakurai, E. Mihaliuk, F. Chirila, and K. Showalter, *Science* **296**, 2009 (2002).
- [21] M. Gassel, E. Glatt, and F. Kaiser, *Phys. Rev. E* **77**, 066220 (2008).
- [22] V. S. Zykov and K. Showalter, *Phys. Rev. Lett.* **94**, 068302 (2005).
- [23] L. Q. Zhou, X. Jia, and Q. Ouyang, *Phys. Rev. Lett.* **88**, 138301 (2002).
- [24] O. Steinbock, J. Schütze, and S. C. Müller, *Phys. Rev. Lett.* **68**, 248 (1992).
- [25] K. I. Agladze and P. De Kepper, *J. Phys. Chem.* **96**, 5239 (1992).
- [26] V. Krinsky, E. Hamm, and V. Voignier, *Phys. Rev. Lett.* **76**, 3854 (1996).
- [27] A. P. Muñuzuri, C. Innocenti, J.-M. Flesselles, J.-M. Gilli, K. I. Agladze, and V. I. Krinsky, *Phys. Rev. E* **50**, R667 (1994).
- [28] J. X. Chen, H. Zhang, and Y. Q. Li, *J. Chem. Phys.* **124**, 014505 (2006).
- [29] L. Y. Deng, H. Zhang, and Y. Q. Li, *Phys. Rev. E* **79**, 036107 (2009).
- [30] Q. Ouyang (private communication).
- [31] R. FitzHugh, *Biophys. J.* **1**, 445 (1961); J. Nagumo, S. Arimoto, and S. Yoshizawa, *Proc. IRE* **50**, 2061 (1962).
- [32] J. J. Taboada, A. P. Muñuzuri, V. Pérez-Muñuzuri, M. Gómez-Gesteira, and V. Pérez-Villar, *Chaos* **4**, 519 (1994).
- [33] M. Gómez-Gesteira, J. Mosquera, V. A. Davydov, V. Pérez-Muñuzuri, A. P. Muñuzuri, V. G. Morozov, and V. Pérez-Villar, *Phys. Lett. A* **231**, 389 (1997).
- [34] See A. S. Mikhailov, V. A. Davydov, and V. S. Zykov, *Physica D (Amsterdam, Neth.)* **70**, 1 (1994), and references therein.
- [35] D. Barkley, *Physica D (Amsterdam, Neth.)* **49**, 61 (1991).
- [36] J. J. Tyson and P. C. Fife, *J. Chem. Phys.* **73**, 2224 (1980).